On the Impact of Different Light Wavelengths in Decoding Human Intention in Lightmyography Controlled Prosthetic Hands

Bonnie Guan[1], Ricardo V. Godoy[1], Anany Dwivedi[2], and Minas Liarokapis[1]

***Abstract*— Lightmyography is a method of human interfacing proposed for the control of prosthetic systems in which light is reflected on the skin and captured using photosensors. While sharing conceptual similarities with forcemyography, lightmyography differentiates itself in the way it interacts with the skin due to skin optics. Different wavelengths of light interact with the skin in different depths and degrees, a principle utilized in photoplethysmography to estimate heart rate and blood oxygen levels. Therefore, lightmyography was previously designed with two wavelengths of light, green and near-infrared. This study seeks to examine the impact of using different wavelengths of light in the decoding of hand postures using different machine learning methods. Four light configurations were tested: using only green light, using only infrared light, using both green and infrared light blinking alternately each 250 ms, and finally using both lights blinking at 125 ms. Data was decoded using four machine learning algorithms, namely linear discriminant analysis, random forest, convolutional neural networks, and a transformer-based model. Statistical testing showed no significant effect from light configuration in the machine learning decoding of hand posture performance. The dataset collected in this study has been made available for further investigation.**

I. Introduction

Electromyography (EMG) is the most widely used method for human-machine interfacing with prosthetic devices [1], [2], [3]. EMG measures electrical activity in muscle movement, and this activity can be interpreted to control prosthetic systems. However, EMG usually incurs high costs due to the specialized equipment required to measure the electrical activity in the muscles. For this reason, other more affordable methods of interfacing are being studied. Forcemyography (FMG) is a method that measures the deformation of the surface of the skin in response to the contraction of the muscles [4], [5]. Meanwhile, mechanomyography (MMG) detects the mechanical vibrations of the skin surface as the muscles move [6]. FMG and MMG require significantly cheaper sensors, however, they are limited to skin surface-level measurements, unlike EMG, which, with even surface electrodes, can measure the electrical activity under the skin at varying depths, based on the distance between electrodes [7]. Sonomyography (SMG) has been proposed, which uses ultrasounds to visualize muscle movements within a cross-sectional area [8]. However, similarly to EMG, SMG uses expensive equipment.

This work was supported by the Ministry of Business, Innovation, and Employment (MBIE), NZ (Grant number: UOW2433).

[1] B. Guan, R. V. Godoy, and M. Liarokapis are with the New Dexterity Research Group, The University of Auckland, Auckland, New Zealand {bgua324, rdeg264}@aucklanduni.ac.nz, minas.liarokapis@auckland.ac.nz

[2] A. Dwivedi is with Te Ipu o te Mahara Artificial Intelligence Institute, University of Waikato, NZ. E-mail: anany.dwivedi@waikato.ac.nz

In our previous work, we proposed a method of human-machine interfacing that we called lightmyography (LMG) [9]. LMG uses photosensors to detect the reflection of light on the skin and muscles, thereby measuring the change in displacement of the muscles. This concept has been applied previously, using near-infrared (NIR) light emitting diodes (LEDs) such as in [10], where the authors used a photo reflector array to produce a wrist contour. The authors in [11] proposed OptoMyoGraphy, which used an NIR armband that showed, by visual inspection, that photosensor recordings would vary for different hand/wrist gestures. Sugiura et al. [12] used NIR photo-reflective sensors on the back of the hand for gesture recognition. These methods focused on the surface shape of the skin. When LMG was proposed, it was theorized that due to the principles of photoplethysmography (PPG) [13], [14], the reflected light could be an indication of not only the skin displacement, but also give insight into biological changes under the skin, such as the flow of blood and muscle or fat density changes. This is because different wavelengths of light penetrate the skin at different depths and also interact differently with the tissue through different absorption and scattering [15]. Based on this theory, LMG employed two wavelengths of light, green light at peak wavelength 525 nm, and IR light at peak wavelength 880 nm, similar to the wavelengths used in PPG devices. Interestingly, despite being used in previous studies to measure skin surface contours, IR wavelengths penetrate the deepest into the skin and thus IR light is commonly used for measuring blood flow in deeper parts of the body, such as the muscles [16], [13].

In this paper we investigate the impact of the use of the two wavelengths, green and IR, implemented previously in LMG. Although it has been shown in research that the two wavelengths of light do penetrate the skin at different depths, it remains unclear as to whether this property is beneficial in the decoding of gestures for prosthesis applications. To explore this, a dataset has been compiled containing photosensor readings with only the green LEDs, only the IR LEDs, both colored LEDs blinking at intervals of 250 ms, and both blinking at 125 ms. Six gestures were recorded from 10 subjects. This dataset is made available at github.com/newdexterity/lmg_wavelength_dataset. Although close analysis of LMG signals may provide insight into muscle and skin deformation, machine learning is widely used in decoding gestures using EMG and FMG. Therefore, we assess the impact of different light penetration depths when classic machine learning and deep learning are employed for the decoding of hand postures.

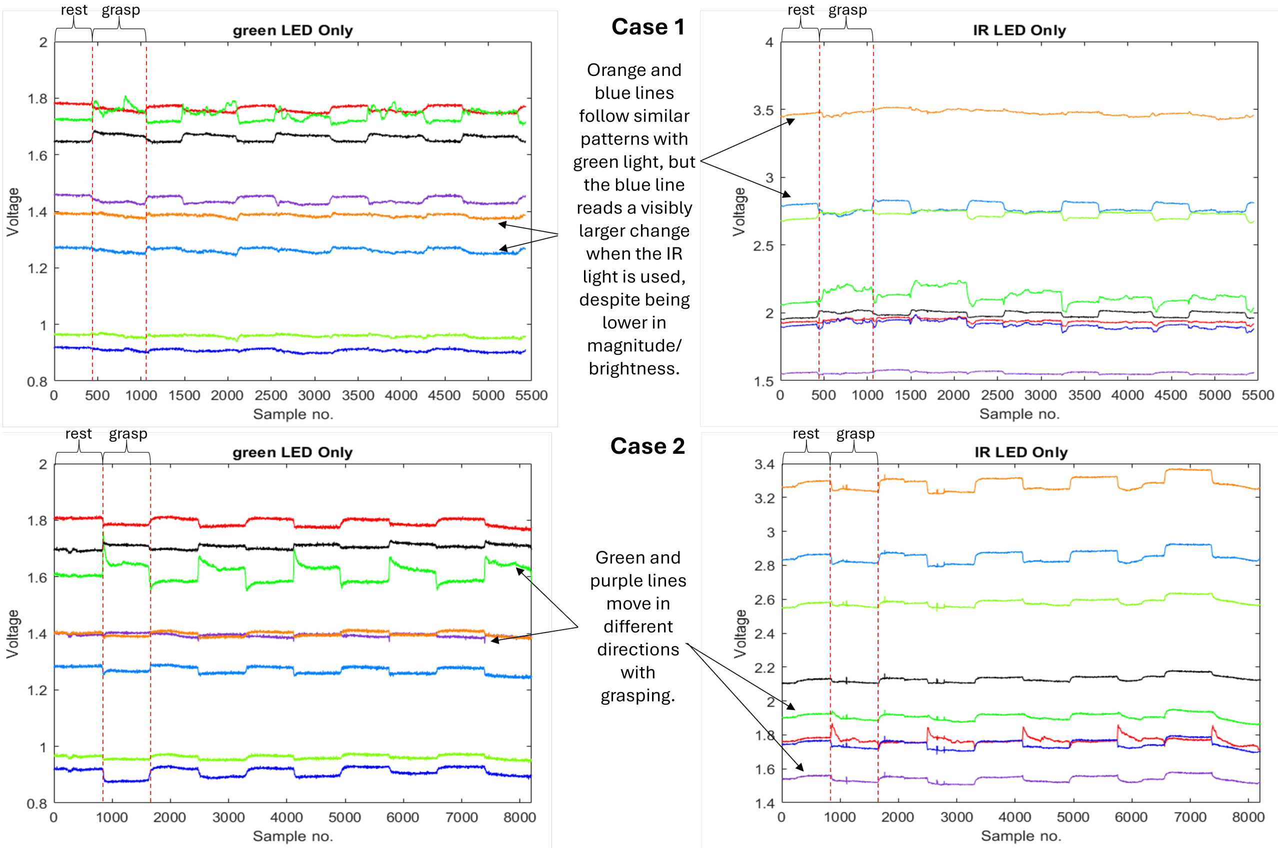

Fig. 1. Visual observations in using green and IR light for the measurement of a full grasp may indicate that the different wavelengths are affected differently by changes in the skin. Measurements were taken from 8 sensors placed on the flexor digitorum superficialis muscle that were not moved between recordings. Cases 1 and 2 are from different subjects, so the sensors' placement is slightly different between cases.

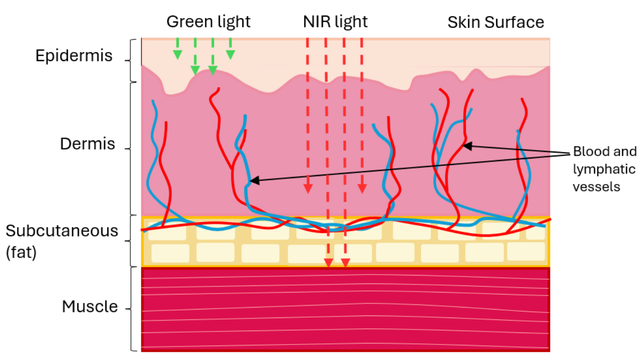

Fig. 2. The layers of the skin. Green light typically penetrates into the epidermis layer, while NIR light can penetrate as far as the muscle, passing through the dermis where many of the blood and lymphatic vessels are.

II. Light Interaction with Skin

The physics of the penetration of light into the skin is already well established in the literature. The tissue in the skin consists of different layers, which each have a range of chromophores that differ in scattering and absorption coefficients depending on the wavelength of light [16], [17], [18]. As light scatters and travels deeper into the skin, the energy density of the wave decreases. Longer wavelengths of light will penetrate further into the skin.

In particular, the 37% of a 500 um (green) light wavelength reduces to approximately 230 µm into the skin while 37% of a wavelength that is 800 nm (NIR) will penetrate to a depth of about 1200 µm [17]. Although the thickness of the skin and its layers varies among individuals, this roughly correlates to the epidermis and the dermis layers in the skin of the arm, with evidence that NIR wavelengths can penetrate as deep as the muscle [19]. The epidermis is a layer composed of a dense layer cells with little blood circulation. A majority of the light radiation is reflected by the top layer of the epidermis. This is especially true in the case when the light source is positioned away from the skin, as the green LED is in the LMG modules. Meanwhile, metabolic exchanges occur in the dermis, which contains networks of blood and lymphatic vessels [20]. It should also be noted that melanin is present mostly in the dermis, which absorbs light, allowing less light to be reflected. An illustration of the skin is shown in Fig. 2. PPG is a measurement technique that utilizes light propagation through or reflected by the tissue. Research in PPG has highlighted some key factors that affect the detected light, including blood volume, oxyhemoglobin, blood vessel contractions and movement, and red blood cell orientation [14]. PPG is widely used in health monitoring systems, such as smart watches, for measuring data such as heart rate and blood oxygen levels [13].

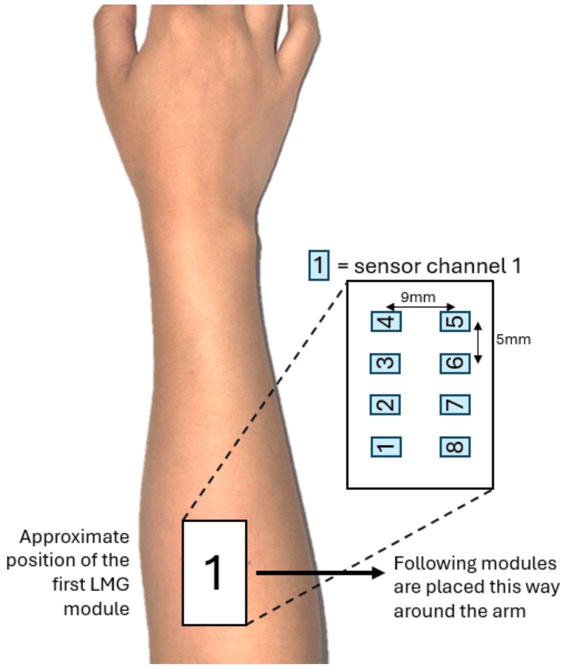

Fig. 3. Approximate placement and channel numbering of the LMG sensors on the arm. Five modules were placed about equally around each subject's arm, with the care to place the first module in the same position for each subject. This means that the size of the participant's arm determines the muscles each module is placed on.

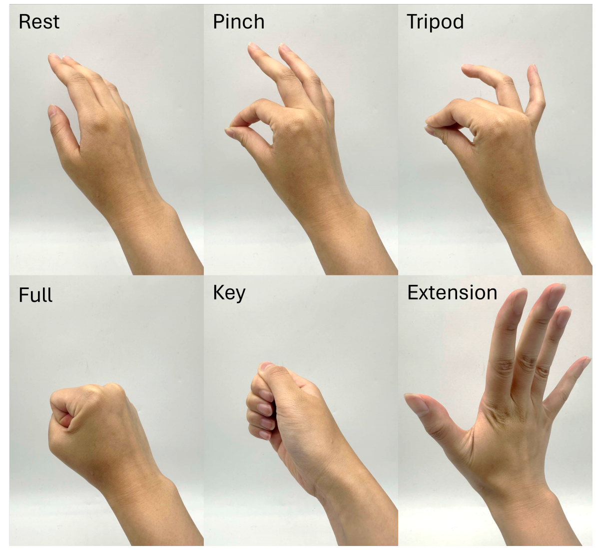

Fig. 4. Four grasps were chosen for decoding based on commonly used everyday grasps, along with rest and extension gestures.

A. Lightmyography

Although green and NIR light waves give varying data, making them valuable in deriving data for health monitoring, they may not have a significant effect on gesture or grasp decoding. Different PPG measuring sites give data with varying degrees of accuracy. Wearable PPG sensors are commonly placed where the skin is thinner or where blood vessels are more dense [13]. However, for the LMG band to detect muscle contractions, it is designed to sit on the forearm, where muscles that are responsible for wrist and finger movement are located. Although NIR has been shown to penetrate as deep as the muscle, this is typically observed with light sources of high power, which is not the case with LMG. Thus, LMG signals may not be able to derive much information about the deformation of the muscles themselves, although blood flow changes through the dermis layer should still influence readings. Moreover, a layer of subcutaneous tissue (fat) is present between the dermis and muscle, which can vary greatly between individuals, further influencing light penetration depth.

A simple test was thus conducted with 3 subjects, each providing written and informed consent to the experimental procedure following ethics guidelines. Data was collected with one LMG module, consisting of 8 sensors, 3 green LEDs, and 2 IR LEDs. This was placed on the forearm, targeting the flexor digitorum superficialis muscle as described in [7]. This muscle requires precise placement of EMG electrodes, as it is often close to other muscles and thus prone to muscle cross-talk. The subjects would perform 5 repetitions of a full grasp for varying amounts of time, with 10 seconds of rest in between. This was first recorded with the IR light, then the green light. To assess repeatability and to ensure consistency in case of fatigue, this procedure was then recorded in reverse order, with the green light first, then the IR light. The sensor was not moved throughout these recordings. Quantitative comparison of green and IR light signals is challenging due to differences in light source power and surface distribution across the surface of the skin. However, some distinct behaviors were visibly observed that indicated the light reflected by the two wavelengths provided different physiological insights. Figure 1 highlights some of these observations. It is still uncertain if these differences contribute to the decoding of gestures.

III. Methods

A. Data Collecion

The University of Auckland Human Participants Ethics Committee (UAHPEC) approved the study with the accepted protocol with reference number #26227. All experiments were performed in accordance with relevant guidelines and regulations. Prior to the study, each subject provided written and informed consent to the experimental procedure. Ten (10) individuals participated in this study. All participants performed experiments with their dominant hand. More information about each subject can be found in Table I. Each participant wore the LMG armband on their forearm. Five (5) LMG modules were spaced approximately equally around the subject's arm, dependent on the forearm size, and no attempt to target a particular muscle was made. This is because if a prosthetic user were to wear the band, they likely would not pay attention to the positioning of the sensors. However, the first module was placed in approximately the same position for every subject, as illustrated in Fig. 3. Visual cues were then given on a computer screen to count

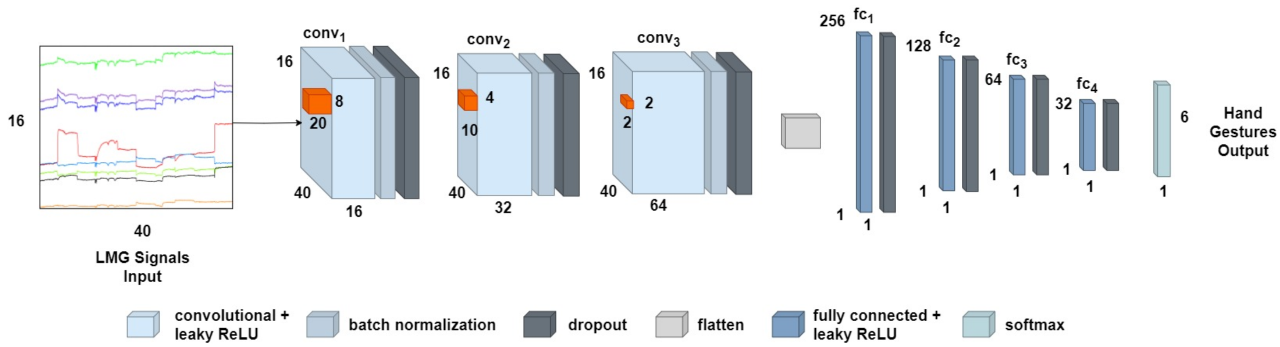

Fig. 5. CNN model for LMG-based gesture decoding. Three convolutional layers are followed by batch normalization and dropout layers. The outputs from the CNN blocks are flattened and provided to four fully-connected layers. A final softmax layer performs the 6-gesture classification.

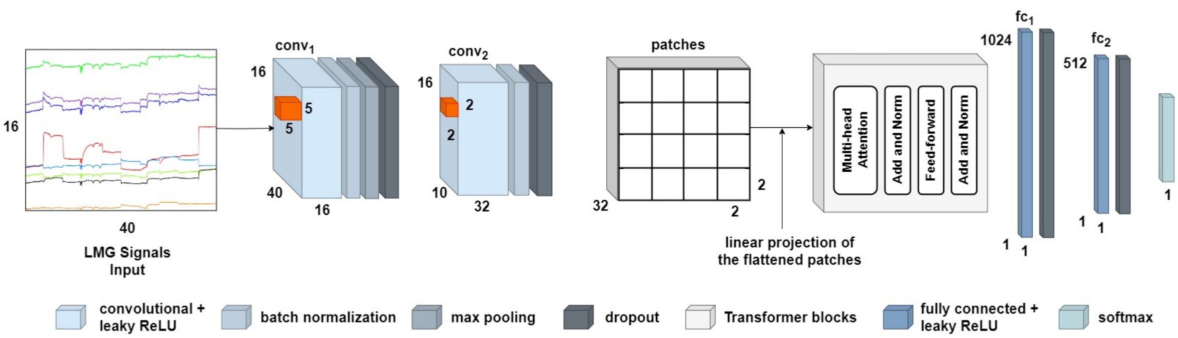

Fig. 6. TMC-ViT Model for LMG data. Two convolution layers extract the embeddings with an embedding size of 32, which are further split into patches of 2×2 and provided to the Transformer block. A final softmax layer with 6 neurons outputs the decoded gesture.

down each transition between rests and grasps whilst also labeling the data collected. Grasps were chosen based on commonly used grasps observed by Bullock et al. [21], along with extension that is a typically more easily distinguishable gesture. The subjects would perform the pinch, tripod, full grasp, key grasp, and extension postures as shown in Fig. 4, in this sequence, for 10 seconds. Ten seconds of rest were performed between each posture. LMG data was collected at a rate of 83 Hz while the participants performed this sequence, which made up one repetition of data. Five repetitions of data were collected for each of the four light configurations: only the green LED, only the IR LED, with both LEDs blinking alternately at 250ms (referred to as *250Both*), and with both LEDs blinking alternately at 125ms (referred to as *125Both*). Subjects placed their wrist on a spongy elevated surface so that neither the hand nor the armband touched the table. They were asked not to move their arm at all for each set of 5 repetitions, however, between sets they were allowed to rest and move their arm with the armband on. The order in which each light configuration was recorded was randomized to prevent fatigue-biased results.

This dataset is made publicly available at: www.github.com/newdexterity/lmg_wavelength_dataset

B. Data Preprocessing

LMG data goes through preprocessing steps before being fed to a machine learning model. We employed a sliding window of 200 ms with a stride of 20 ms to extract samples from the LMG data collected. The sliding window was chosen to be larger than 125 ms to avoid high biases and variance [22] and smaller than 300 ms due to real-time constraints of prosthetic control systems [23]. The data was balanced as the rest class is most prevalent. This guarantees that we have the same number of samples for each of the 6 classes and avoids bias toward a particular class. To do so, we randomly downsampled the majority classes until each class presented the same number of instances. Batch normalization layers within the deep learning models incorporates normalization into the architecture, and no normalization was needed for classical machine learning methods.

TABLE I

SUBJECTS' INFORMATION. *M* STANDS FOR MALE, *F* FOR FEMALE, AND *Hand.* FOR HANDEDNESS.

Subject	**1**	**2**	**3**	**4**	**5**	**6**	**7**	**8**	**9**	**10**
Sex	F	M	M	M	M	F	M	M	M	M
Hand.	Right	Right	Right	Right	Right	Left	Right	Left	Right	Right
Age	26	31	24	25	24	24	27	27	27	35

C. Classic Machine Learning Models

Two classical machine learning methods were employed for decoding the data. Linear discriminant analysis (LDA) [25], which is a common method applied in decoding FMG [26]. Along with random forest (RF) [27], which is more popular among EMG decoding [28]. LDA is a method of dimensionality reduction that projects data such that classes are separated in the new dimensionality. RFs are

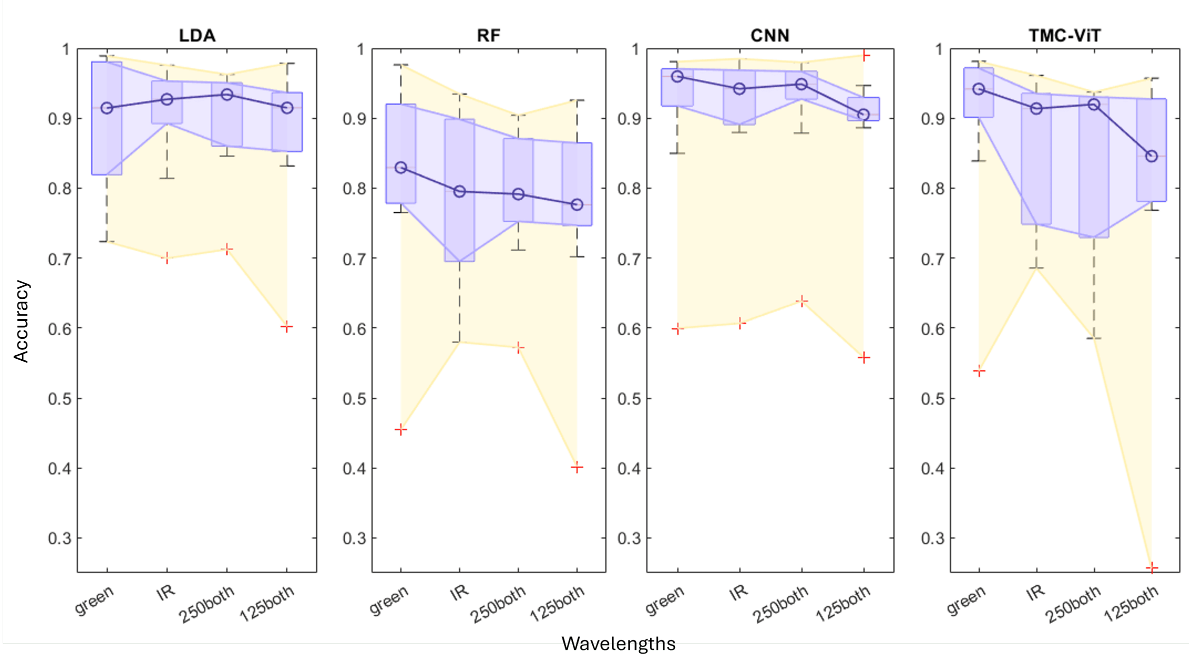

Fig. 7. Boxplots zones [24] of the accuracies achieved with each wavelength and machine learning model. There was no significant difference in any light configuration. RF performed significantly worse than all other models, while CNN performed significantly better than TMC-ViT. No significant difference was found between CNN and LDA decoding, or LDA and TMC-ViT decoding.

an ensemble learning method for classification and regression that works by constructing multiple decision trees at training time. The output of RF is then determined by the majority vote among the trees, which enhances accuracy by averaging across several deep decision trees and reducing overfitting risks. The RF model comprised of 100 trees. Both methods were implemented using the scikit-learn python package.

D. Deep Learning Models

Two deep learning methods were also chosen for decoding. The convolutional neural network (CNN) [29] was chosen as they have been employed in several applications due to their ability to extract spatial characteristics and identify patterns of a given input data. More information about the employed CNN model can be seen in Fig. 5. The second deep learning technique employed for decoding LMG signals was the Temporal Multi-Channel Vision Transformers (TMC-ViT) [30]. This technique was chosen based on evidence from our previous works, which showed that the TMC-ViT outperformed the well-established machine learning techniques such as CNN and RF [9], especially for EMG decoding purposes [31]. The TMC-ViT is a Transformer-based model that adapts the Vision Transformer [32] to process temporal data with multiple channels, employing convolutional layers to extract its embeddings. More information about the employed TMC-ViT model can be seen in Fig. 6. Deep Learning models were implemented using Keras and TensorFlow python packages. For these models, the loss function was the sparse categorical cross-entropy. Optimization was performed using Adam [33].

IV. Results and Discussion

All the machine learning models were validated using 5-fold cross-validation. The average of each 5 folds was calculated for each model, wavelength configuration, and subject. Overall results are plotted in Fig. 7 while Table II shows each subject's results. Note that the means of the boxplots do not include the outliers and differ from the means in the table.

A two-way repeated measures ANOVA [34] revealed a main effect of classifier ($p<0.001$), whereas the main effect of light condition was not statistically significant ($p=0.245$). Furthermore, the interaction between classifier and light condition was non-significant ($p=0.392$). These findings indicate that, overall, the choice of classifier substantially influences decoding performance, while the specific light wavelength condition does not.

Post hoc pairwise comparisons (Bonferroni-corrected) [35] further clarified these differences. The RF classifier performed significantly worse than the other classifiers: RF's accuracy was lower than that of CNN ($p<0.001$), LDA ($p=0.00032$), and TMC-ViT ($p=0.00371$). Notably, the comparison between CNN and LDA yielded a very small difference that was not significant, indicating that these two methods perform similarly. However, CNN was found to significantly outperform TMC-ViT ($p=0.00766$), whereas the difference between LDA and TMC-ViT was not significant. This differs from our previous research in which TMC-ViT performed well in comparison [36]. This is likely due to different data collection methods, as previously, all repetitions of one grasp/class were performed sequentially, leading to less variation in the data and, thus, easier decoding. However,

TABLE II

THE AVERAGE (AVE) ACCURACIES OF EACH SUBJECT (SUBJ), MODEL, AND LIGHT CONFIGURATION, EXPRESSED AS A PERCENTAGE.

	LDA				RF				CNN				ViT			
subj	green	ir	250b	125b	green	ir	250b	125b	green	ir	250b	125b	green	ir	250b	125b
1	89.98	93.29	86	83.17	80.53	79.48	78.88	77.36	93.55	94.15	87.86	89.65	90.12	90.17	58.53	78.11
2	98.89	96.2	93.19	97.82	97.63	89.83	77.04	87.95	98.07	98.3	97.15	98.98	98.04	93.51	93.03	92.73
3	81.94	81.38	87.39	85.26	80.15	69.53	75.24	74.69	91.76	87.96	92.75	88.63	92.66	70.63	84.86	83.53
4	98.18	89.26	84.57	88.58	92.01	82.95	79.4	85.67	96.2	96.49	93.05	94.67	98.11	93.43	91.56	95.7
5	72.35	69.97	71.24	60.22	45.47	57.99	57.23	40.17	59.95	60.66	63.85	55.83	53.85	68.57	59.37	25.64
6	98.03	95.3	96.06	95.91	86.09	71.29	89	70.2	97.48	91.87	97.97	90.17	94.45	88.16	72.97	83.23
7	79.83	92.1	96.24	93.63	76.51	67.81	90.41	86.45	84.97	89.1	94.62	90.29	83.89	74.87	93.63	90.97
8	95.12	90.58	94.5	91.45	93.45	93.45	87.07	77.91	95.72	96.85	95.47	90.71	97.15	94.43	93.02	76.83
9	88.84	93.57	93.56	91.48	77.87	79.56	86.16	92.56	97.06	94.25	96.67	92.94	96.39	92.56	93.72	93.85
10	92.92	97.57	95.05	93.47	85.35	91.62	71.14	76.99	96.84	98.49	95.1	92.66	93.9	96.1	92.37	85.59
Ave	89.61	89.92	89.78	88.1	81.5	78.35	79.16	76.99	91.16	90.81	91.45	88.45	89.86	86.24	83.31	80.62

this previous method was not robust when applied practically, as the arm posture will move over time, affecting the signals.

The analysis of the light condition factor showed no significant differences across the four wavelengths. The pairwise comparisons among green, IR, 250both, and 125both all produced non-significant differences ($p>0.322$). This lack of significance suggests that, under the current experimental conditions, the decoding accuracy is robust to changes in the light wavelength. In practical terms, the choice among these light conditions does not appear to be critical for the performance of the classifiers.

A. Limitations and Design Considerations for Prosthesis

It should be noted that in these experiments, there were no significant differences between light configurations, and they did not significantly affect machine learning decoding accuracy. Moreover, we have not fully investigated the effect of light wavelength on gesture recognition, and we have not fully explored the differences between LMG and FMG. This is because, firstly, this study only decodes 6 classes. It is possible that when decoding a larger number of classes, the wavelength configuration will have a more significant effect, especially between similar classes. However, we must keep in mind that increasing the number of classes will increase data collection times, making it less practical for prothesis applications. If designing for a control system where decoding a high number of classes is not necessary, there is no need to design for the use of varying wavelengths, as any effect, if any, is likely negligible to the decoding. Secondly, only limited machine learning methods were explored for the decoding of gestures, but there may be analytical methods to be developed that can leverage techniques from PPG measuring. For example, for the measuring of heart rate, signals are broken into DC and AC components [37]. Other machine learning methods may also be more suitable. Additionally, feature extraction methods, such as those applied in FMG studies [38], may also reveal more information when both wavelengths are used. Authors encourage others to look at the dataset themselves to give their own insights. Thirdly, the current LMG modules are designed so that the photosensors read both green and IR wavelengths, thus the need to blink between the two coloured LEDs. However, the LMG module could also be designed with some photosensors that only detect green wavelengths and some IR wavelengths to give cleaner signals with no need to alternate between the two LEDs. CNN and LDA models outperformed the RF model, and CNN outperformed the TMC-ViT model. This is seen similarly in FMG studies where LDA shows comparable or better performance to more complex models [39], indicating that raw LMG signals are simple and using overcomplex models is likely not suitable for LMG decoding. LDA is also a popular choice due to its efficient learning and lightweight computational power, making it suitable for embedded design.

V. CONCLUSION

This paper investigates the use of different wavelengths of light for use in lightmyography-based decoding with machine learning models. To do so, lightmyography data was collected from 10 subjects performing 6 classes, while varying light configurations were applied: with only green LEDs on, with only IR LEDs on, with both green and IR LEDs blinking alternately every 250 ms, and with both LEDs blinking at 125 ms. This dataset is made publicly available for other researchers to investigate. Four machine learning algorithms were trained to decode the grasp postures and gestures, and their results were analyzed for statistical differences. Results showed that there was no significant effect of the light wavelengths on the decoding of hand postures with these 4 machine learning methods. However, decoding with random forest models yields significantly lower decoding accuracies compared to all other methods. Additionally, no significant difference was observed between decoding using linear discriminant analysis with temporal multi-channel vision transformers or convolutional neural networks. However, convolutional neural networks did perform significantly better than the temporal multi-channel vision transformers. Therefore, although there may be other methods of decoding that may be influenced by additional light wavelengths, future lightmyography developments likely do not need to consider this if decoding with simple machine learning methods.

REFERENCES

[1] M. Zecca, S. Micera, M. C. Carrozza, and P. Dario, "Control of multifunctional prosthetic hands by processing the electromyographic signal," *Critical Reviews™ in Biomedical Engineering*, vol. 30, no. 4-6, 2002.

[2] C. Castellini and P. Van Der Smagt, "Surface emg in advanced hand prosthetics," *Biological cybernetics*, vol. 100, pp. 35–47, 2009.

[3] J. O. d. O. de Souza, M. D. Bloedow, F. C. Rubo, R. M. de Figueiredo, G. Pessin, and S. J. Rigo, "Investigation of different approaches to real-time control of prosthetic hands with electromyography signals," *IEEE Sensors Journal*, vol. 21, no. 18, pp. 20 674–20 684, 2021.

[4] A. Prakash, A. K. Sahi, N. Sharma, and S. Sharma, "Force myography controlled multifunctional hand prosthesis for upper-limb amputees," *Biomedical Signal Processing and Control*, vol. 62, p. 102122, 2020.

[5] E. Cho, R. Chen, L.-K. Merhi, Z. Xiao, B. Pousett, and C. Menon, "Force myography to control robotic upper extremity prostheses: a feasibility study," *Frontiers in bioengineering and biotechnology*, vol. 4, p. 18, 2016.

[6] S. Wilson and R. Vaidyanathan, "Upper-limb prosthetic control using wearable multichannel mechanomyography," in *2017 International Conference on Rehabilitation Robotics (ICORR)*. IEEE, 2017.

[7] E. Criswell, "Cram's introduction to surface electromyography," *Jones &Bartlett Learning*, 2010.

[8] V. Nazari and Y.-P. Zheng, "Controlling upper limb prostheses using sonomyography (smg): A review," *Sensors*, vol. 23, no. 4, 2023.

[9] M. Shahmohammadi, B. Guan, R. V. Godoy, A. Dwivedi, P. Nielsen, and M. Liarokapis, "On lightmyography based muscle-machine interfaces for the efficient decoding of human gestures and forces," *Scientific Reports*, vol. 13, no. 1, p. 327, 2023.

[10] R. Fukui, M. Watanabe, T. Gyota, M. Shimosaka, and T. Sato, "Hand shape classification with a wrist contour sensor: development of a prototype device," in *Proceedings of the 13th international conference on Ubiquitous computing*, 2011, pp. 311–314.

[11] H. H. Muhammed and R. Jammalamadaka, "A new approach for rehabilitation and upper-limb prosthesis control using optomyography (omg)," in *2016 1st International Conference on Biomedical Engineering (IBIOMED)*. IEEE, 2016, pp. 1–6.

[12] Y. Sugiura, F. Nakamura, W. Kawai, T. Kikuchi, and M. Sugimoto, "Behind the palm: Hand gesture recognition through measuring skin deformation on back of hand by using optical sensors," in *2017 56th Annual Conference of the Society of Instrument and Control Engineers of Japan (SICE)*. IEEE, 2017, pp. 1082–1087.

[13] D. Castaneda, A. Esparza, M. Ghamari, C. Soltanpur, and H. Nazeran, "A review on wearable photoplethysmography sensors and their potential future applications in health care," *International journal of biosensors & bioelectronics*, vol. 4, no. 4, p. 195, 2018.

[14] J. Allen, "Photoplethysmography and its application in clinical physiological measurement," *Physiological measurement*, vol. 28, no. 3, p. R1, 2007.

[15] J. Dawson, D. Barker, D. Ellis, J. Cotterill, E. Grassam, G. Fisher, and J. Feather, "A theoretical and experimental study of light absorption and scattering by in vivo skin," *Physics in Medicine & Biology*, vol. 25, no. 4, p. 695, 1980.

[16] C. Ash, M. Dubec, K. Donne, and T. Bashford, "Effect of wavelength and beam width on penetration in light-tissue interaction using computational methods," *Lasers in medical science*, vol. 32, 2017.

[17] R. R. Anderson and J. A. Parrish, "The optics of human skin," *Journal of investigative dermatology*, vol. 77, no. 1, pp. 13–19, 1981.

[18] S.-H. Tseng, P. Bargo, A. Durkin, and N. Kollias, "Chromophore concentrations, absorption and scattering properties of human skin invivo," *Optics express*, vol. 17, no. 17, pp. 14 599–14 617, 2009.

[19] A. Currà, R. Gasbarrone, A. Cardillo, C. Trompetto, F. Fattapposta, F. Pierelli, P. Missori, G. Bonifazi, and S. Serranti, "Near-infrared spectroscopy as a tool for in vivo analysis of human muscles," *Scientific Reports*, vol. 9, no. 1, p. 8623, 2019.

[20] J.-L. Cracowski and M. Roustit, "Human skin microcirculation," *Compr Physiol*, vol. 10, no. 3, pp. 1105–1154, 2020.

[21] I. M. Bullock, J. Z. Zheng, S. De La Rosa, C. Guertler, and A. M. Dollar, "Grasp frequency and usage in daily household and machine shop tasks," *IEEE transactions on haptics*, vol. 6, no. 3, 2013.

[22] M. Asghari Oskoei and H. Hu, "Myoelectric control systems—a survey," *Biomedical Signal Processing and Control*, vol. 2, no. 4, 2007.

[23] K. Englehart, B. Hudgin, and P. Parker, "A wavelet-based continuous classification scheme for multifunction myoelectric control," *IEEE Transactions on Biomedical Engineering*, vol. 48, 2001.

[24] M. V. Liarokapis, P. K. Artemiadis, P. T. Katsiaris, K. J. Kyriakopoulos, and E. S. Manolakos, "Learning human reach-to-grasp strategies: Towards emg-based control of robotic arm-hand systems," in *2012 IEEE International Conference on Robotics and Automation*. IEEE, 2012.

[25] R. A. Fisher, "The use of multiple measurements in taxonomic problems," *Annals of eugenics*, vol. 7, no. 2, pp. 179–188, 1936.

[26] O. Sherif, M. M. Bassuoni, and O. Mehrez, "A survey on the state of the art of force myography technique (fmg): analysis and assessment," *Medical & Biological Engineering & Computing*, vol. 62, no. 5, pp. 1313–1332, 2024.

[27] T. K. Ho, "Random decision forests," in *Proceedings of 3rd international conference on document analysis and recognition*. IEEE, 1995.

[28] S. A. Syed, H. Zahid, S. Bullo, S. Shams, S. Tanvir, S. J. H. Zaidi, and S. Nasim, "Machine learning techniques applied in surface emg detection-a systematic review," *Pakistan Journal of Biotechnology*, vol. 20, no. 02, pp. 225–237, 2023.

[29] Y. LeCun, Y. Bengio *et al.*, "Convolutional networks for images, speech, and time series," *The handbook of brain theory and neural networks*, vol. 3361, no. 10, p. 1995, 1995.

[30] R. V. Godoy, G. J. G. Lahr, A. Dwivedi, T. J. S. Reis, P. H. Polegato, M. Becker, G. A. P. Caurin, and M. Liarokapis, "Electromyography-based, robust hand motion classification employing temporal multichannel vision transformers," *IEEE Robotics and Automation Letters*, vol. 7, no. 4, pp. 10 200–10 207, 2022.

[31] R. V. Godoy, G. J. Lahr, A. Dwivedi, T. J. Reis, P. H. Polegato, M. Becker, G. A. Caurin, and M. Liarokapis, "Electromyography-based, robust hand motion classification employing temporal multichannel vision transformers," *IEEE Robotics and Automation Letters*, vol. 7, no. 4, 2022.

[32] A. Dosovitskiy, L. Beyer, A. Kolesnikov, D. Weissenborn, X. Zhai, T. Unterthiner, M. Dehghani, M. Minderer, G. Heigold, S. Gelly, J. Uszkoreit, and N. Houlsby, "An image is worth 16x16 words: Transformers for image recognition at scale," 2020. [Online]. Available: https://arxiv.org/abs/2010.11929

[33] D. P. Kingma and J. Ba, "Adam: A Method for Stochastic Optimization," *3rd International Conference on Learning Representations, ICLR 2015 - Conference Track Proceedings*, pp. 1–15, dec 2014.

[34] T. D. Wickens and G. Keppel, *Design and analysis: A researcher's handbook*. Pearson Prentice-Hall Upper Saddle River, NJ, 2004.

[35] J. Hsu, *Multiple comparisons: theory and methods*. CRC Press, 1996.

[36] R. V. Godoy, A. Dwivedi, M. Shahmohammadi, and M. Liarokapis, "Lightmyography based decoding of human intention using temporal multi-channel transformers," in *2022 IEEE/RSJ International Conference on Intelligent Robots and Systems (IROS)*. IEEE, 2022.

[37] N. Saquib, M. T. I. Papon, I. Ahmad, and A. Rahman, "Measurement of heart rate using photoplethysmography," in *2015 International Conference on Networking Systems and Security (NSysS)*. IEEE, 2015, pp. 1–6.

[38] Z. G. Xiao and C. Menon, "Counting grasping action using force myography: an exploratory study with healthy individuals," *JMIR Rehabilitation and Assistive technologies*, vol. 4, no. 1, p. e6901, 2017.

[39] ——, "A review of force myography research and development," *Sensors*, vol. 19, no. 20, p. 4557, 2019.